Electronic Supplementary Material (ESI) for Physical Chemistry Chemical Physics

Supporting Information

New Doping Strategy in Hematite Photoanode for Solar Water Splitting: Oxygen Vacancy Generation

Tae-Youl Yang, Ho-Young Kang, Uk Sim, Young-Joo Lee, Ji-Hoon Lee, Byungjin Koo, Ki Tae Nam,* and Young-Chang Joo*

Department of Materials Science and Engineering, Seoul National University, Gwanak-ro 1, Gwanak-gu, Seoul 151-744, Republic of Korea

*Corresponding author:

Prof. Young-Chang Joo

E-mail: ycjoo@snu.ac.kr

Seoul National University, Korea

Prof. Ki Tae Nam

E-mail: nkitae@snu.ac.kr

Seoul National University, Korea

1. Preparation of hematite films

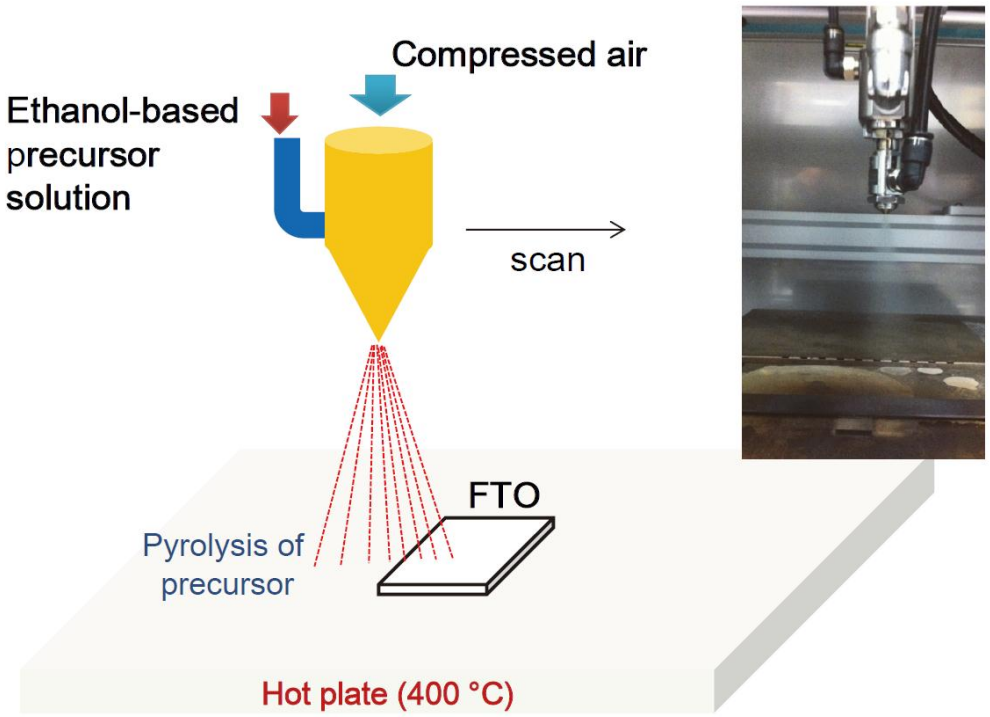

Figure S1. The aerosol spray pyrolysis (ASP) method for the preparation of hematite films.

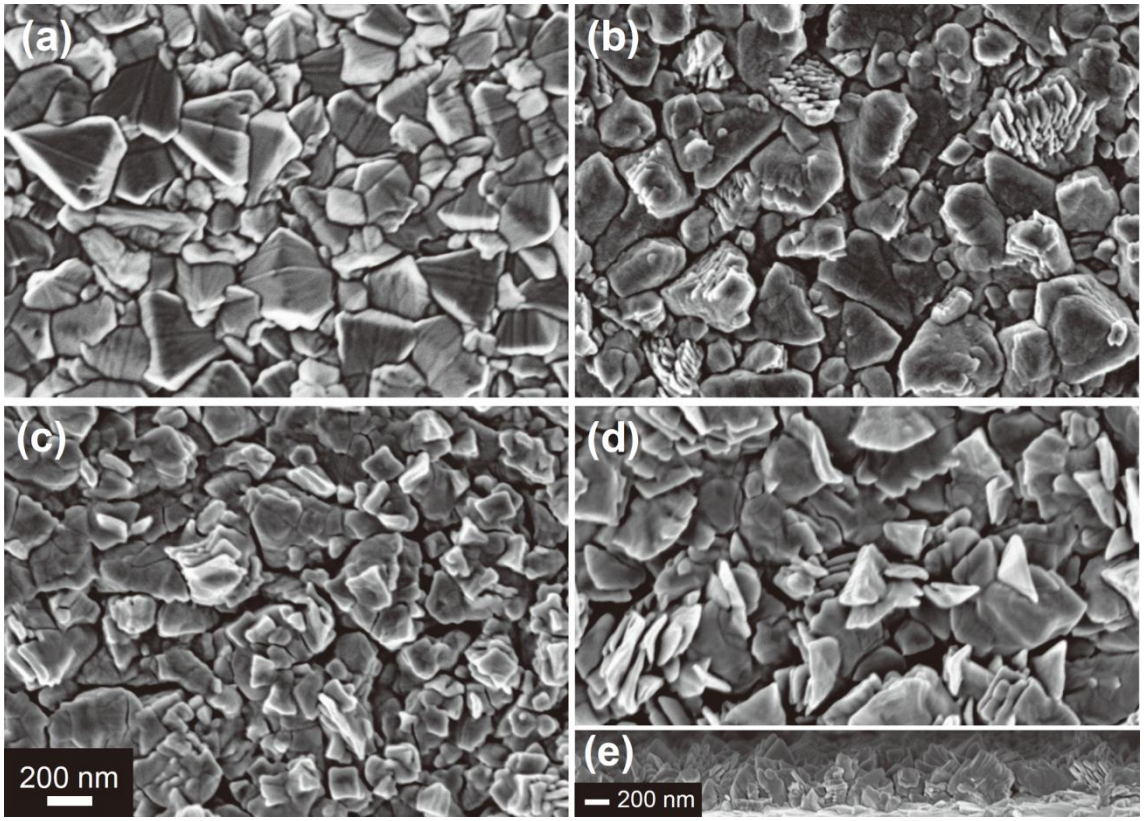

Figure S2. Scanning electron microscopy (SEM) images of (a) the FTO substrate and the hematite films formed by the spraying of an $FeCl_3$-ethanol precursor solution with a volume of (b) 30 mL, (c) 60 mL, and (d) 90 mL. (e) Cross-sectional SEM of hematite films formed by the spraying of the 90mL-solution.

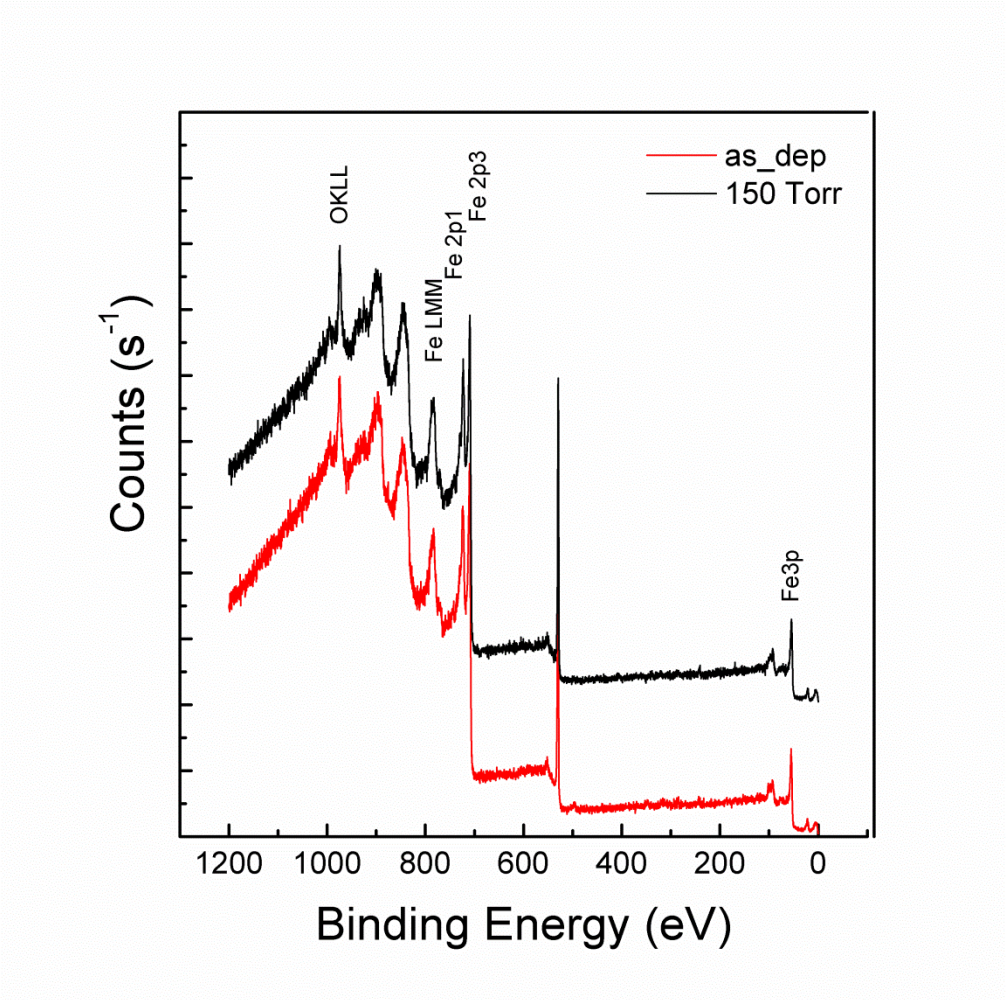

Figure S3. X-ray photoelectron spectroscopy **(**XPS) spectra measured from the as-coated hematite (red) and from the hematite after thermal reduction and oxidative annealing at ambient air (pO_2 = 150 Torr)(black).

2. Post annealing process

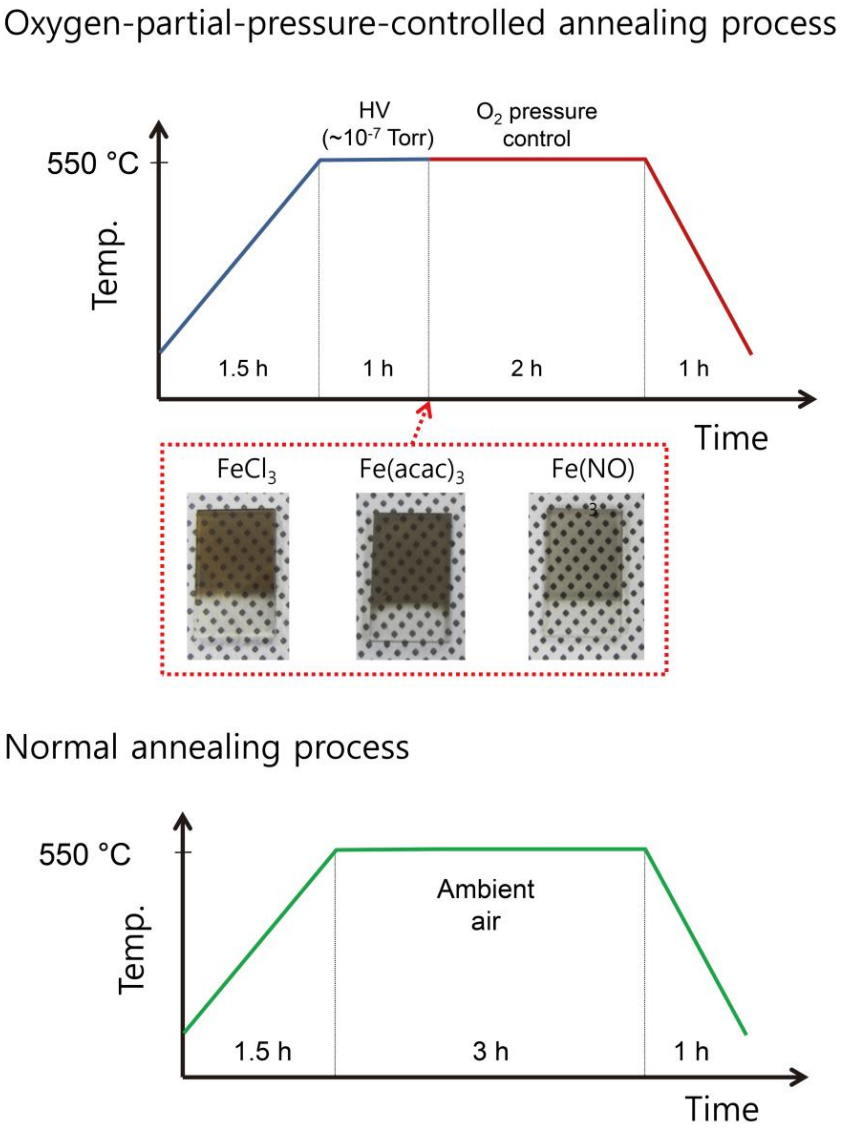

Figure S4. Annealing procedure and atmospheric conditions for oxygen-partial-pressure-controlled annealing and for normal annealing. Photographs for reduced magnetite films prepared from the different precursors and after HV annealing: ferric chloride ($FeCl_3$), ferric acetylacetonate ($Fe(acac)_3$), and ferric nitrate ($Fe(NO_3)_3$).

3. Measurement of photocurrent in hematite

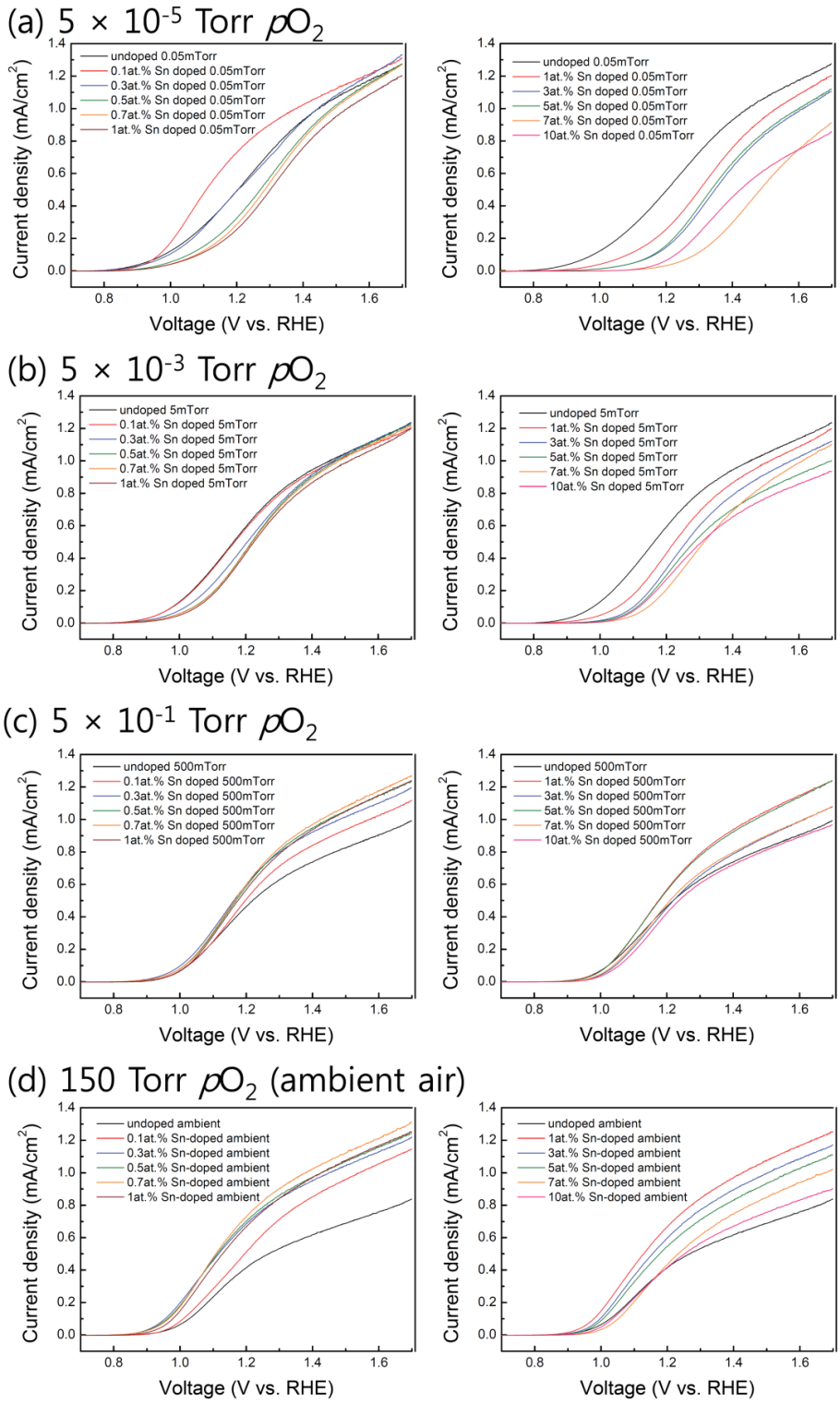

Figure S5. Photocurrent density–potential (J–V) curves for hematite films with different Sn-doping concentrations annealed under controlled oxygen partial pressures.

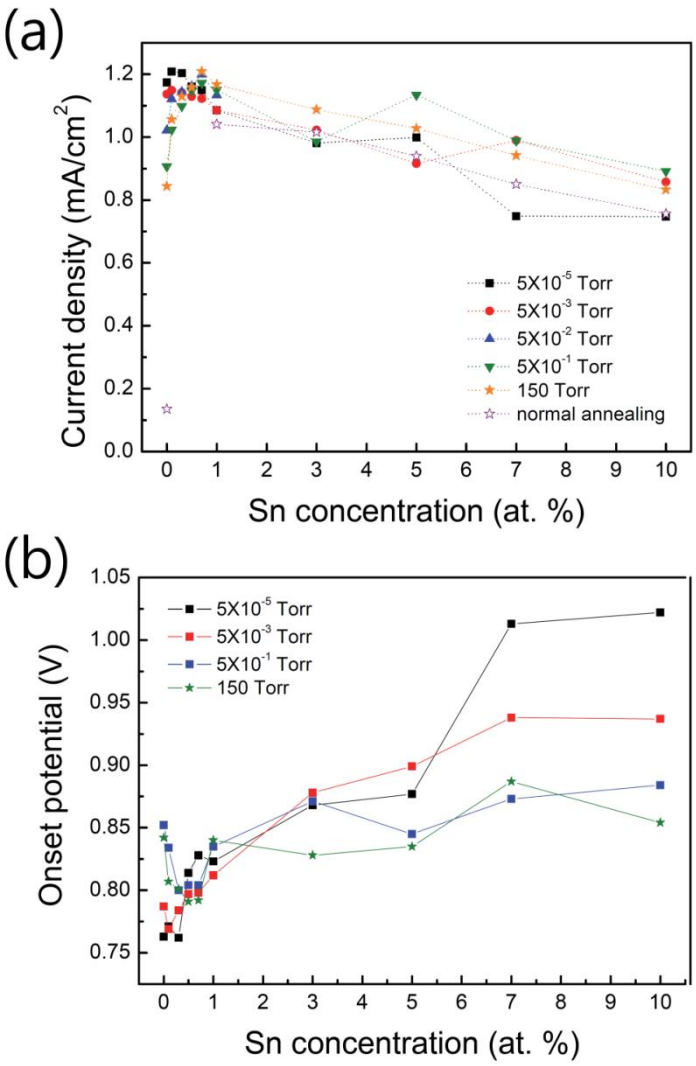

Figure S6. (a) Photocurrent density at 1.6 V vs. RHE. (b) Photocurrent onset potential for hematite films after pO_2-controlled annealing with various pO_2 levels as a function of the doping concentration (0.1 at.% ~ 10 at. %).

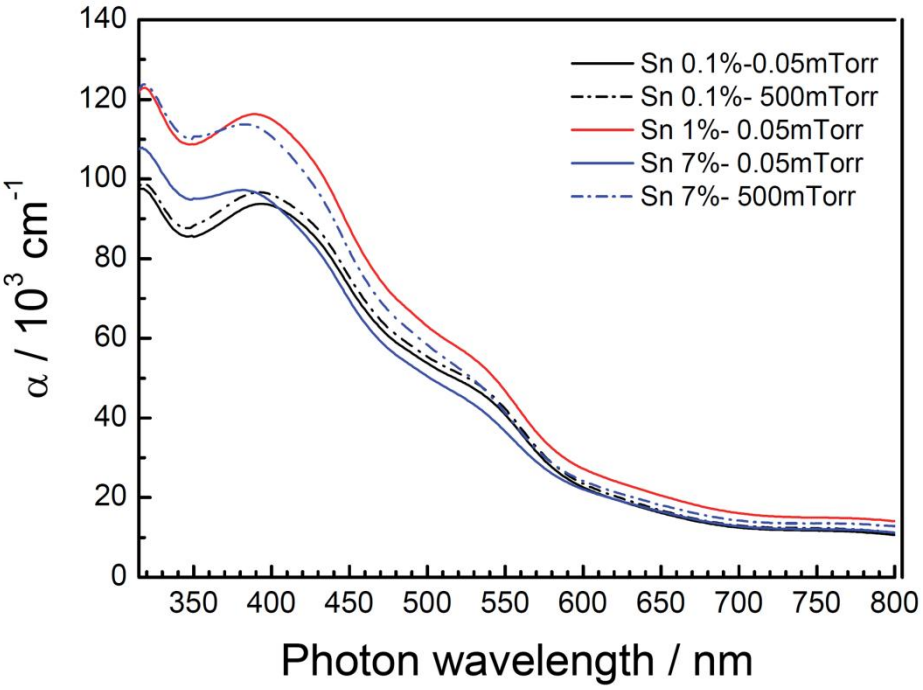

Figure S7. Optical property of hematite films in the various pO_2 and Sn concentration, which shows the absorption coefficient as a function of wavelength. The optical property of hematite, absorption, did not affect the photoactivity in hematite. The absorption coefficient of 0.1% Sn-doped hematite was not changed by the ambient during the post-annealing (See solid black line and dash-dotted black line). Doping concentration has little influence on absorption. The peaks near 390 nm, which arise from a ligand-to-metal charge transfer ($6t_{1u}\downarrow \rightarrow 2t_{2g}\downarrow$), are blue-shifted in the samples with higher Sn-concentration. Although 1 at.% Sn-doped sample shows the highest value of absorption coefficient, this can result from the difference in film thickness. Indeed, 7 at.% Sn-doped sample annealed at 5×10^{-1} Torr (dash-dotted blue line) shows the higher absorption coefficient than 0.1 at.% Sn-doped sample annealed at 5×10^{-1} Torr (dash-dotted black line), but the photocurrent density is higher in the 0.1 at.% Sn-doped hematite.

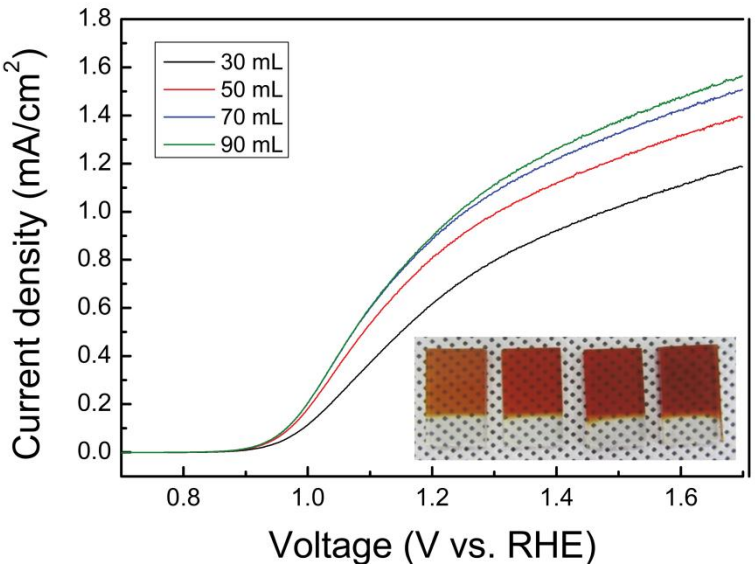

Figure S8. Photocurrent density–potential (J–V) curves for 1at.%-Sn-doped hematite film annealed at 150 Torr-pO_2 (ambient air) in various amount of precursor solution. Inset: photographs for hematite photoanode prepared by ASP using 30 mL, 50 mL, 70 mL, and 90 mL of precursor solution.